Article

Cell Reports

The Microcephaly-Associated Protein Wdr62/CG7337 Is Required to Maintain Centrosome Asymmetry in *Drosophila* Neuroblasts

Graphical Abstract

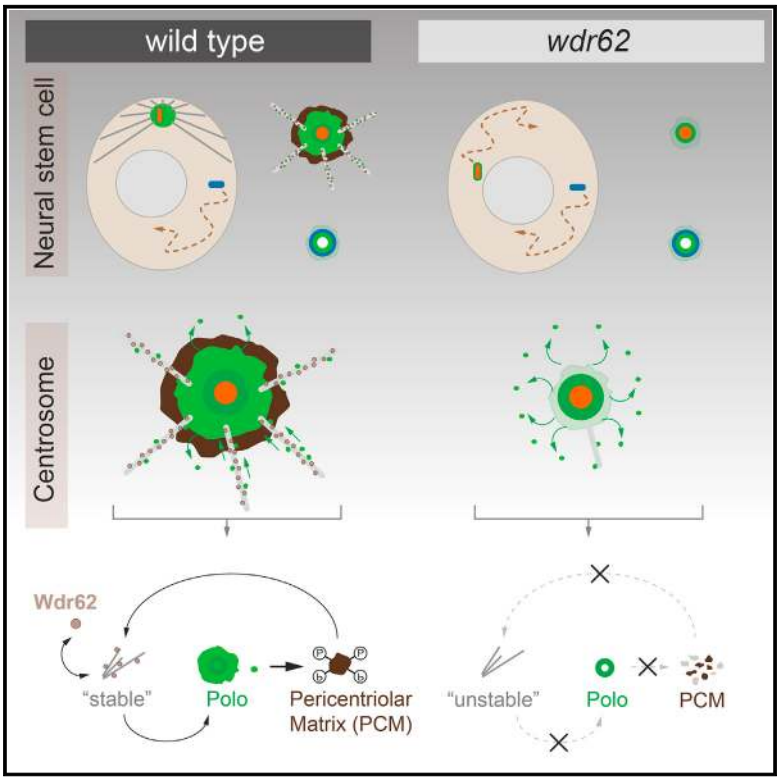

Authors

Anjana Ramdas Nair, Priyanka Singh, David Salvador Garcia, David Rodriguez-Crespo, Boris Egger, Clemens Cabernard

Correspondence

clemens.cabernard@unibas.ch

In Brief

The molecular mechanisms underlying centrosome asymmetry and its function are unclear. Ramdas Nair et al. report that CG7337/Wdr62, previously implicated in the neurodevelopmental disorder microcephaly, maintains centrosome asymmetry in *Drosophila* neural stem cells by stabilizing interphase microtubules. Independently of this function, Wdr62 also regulates cell-cycle progression.

Highlights

- CG7337/Wdr62 maintains centrosome asymmetry in *Drosophila* neural stem cells
- Wdr62 stabilizes interphase microtubules
- Interphase microtubules recruit the mitotic kinase Polo/Plk1 to the centrosome
- Centrosome asymmetry controls spindle orientation and centrosome segregation

Ramdas Nair et al., 2016, Cell Reports *14*, 1100–1113
February 9, 2016
http://dx.doi.org/10.1016/j.celrep.2015.12.097

CellPress

OPEN ACCESS
CellPress

Cell Reports
Article

The Microcephaly-Associated Protein Wdr62/CG7337 Is Required to Maintain Centrosome Asymmetry in *Drosophila* Neuroblasts

Anjana Ramdas Nair,[1] Priyanka Singh,[1,3] David Salvador Garcia,[1] David Rodriguez-Crespo,[2] Boris Egger,[2] and Clemens Cabernard[1,*]

[1]Biozentrum, University of Basel, Klingelbergstrasse 50-70, 4056 Basel, Switzerland
[2]Department of Biology, University of Fribourg, Chemin du Musée 10, 1700 Fribourg, Switzerland
[3]Present address: Department of Mechanistic Cell Biology, Max-Planck Institute of Molecular Physiology, Otto-Hahn-Strasse 11, 44227 Dortmund, Germany
*Correspondence: clemens.cabernard@unibas.ch
http://dx.doi.org/10.1016/j.celrep.2015.12.097

SUMMARY

Centrosome asymmetry has been implicated in stem cell fate maintenance in both flies and vertebrates, but the underlying molecular mechanisms are incompletely understood. Here, we report that loss of CG7337, the fly ortholog of WDR62, compromises interphase centrosome asymmetry in fly neural stem cells (neuroblasts). Wdr62 maintains an active interphase microtubule-organizing center (MTOC) by stabilizing microtubules (MTs), which are necessary for sustained recruitment of Polo/Plk1 to the pericentriolar matrix (PCM) and downregulation of Pericentrin-like protein (Plp). The loss of an active MTOC in *wdr62* mutants compromises centrosome positioning, spindle orientation, and biased centrosome segregation. *wdr62* mutant flies also have an ~40% reduction in brain size as a result of cell-cycle delays. We propose that CG7337/Wdr62, a microtubule-associated protein, is required for the maintenance of interphase microtubules, thereby regulating centrosomal Polo and Plp levels. Independent of this function, Wdr62 is also required for the timely mitotic entry of neural stem cells.

INTRODUCTION

Centrosomes, microtubule (MT)-organizing centers (MTOCs) of metazoan cells, segregate asymmetrically in both fly and vertebrate neural stem cells and have been implicated in stem cell fate maintenance (Yamashita et al., 2007; Conduit and Raff, 2010; Januschke et al., 2011; Wang et al., 2009; Salzmann et al., 2014). The building blocks of centrosomes are centrioles, cylindrical MT-based structures ensheathed by pericentriolar matrix (PCM) proteins (Nigg and Stearns, 2011). Centrosomes are intrinsically asymmetric since centrioles replicate semi-conservatively, generating an older mother centriole and a younger daughter centriole. Centrosome asymmetry is also manifested in the localization of daughter or mother centriole-specific centrosome markers and differential MTOC activity (Januschke et al., 2011, 2013; Rusan and Peifer, 2007; Rebollo et al., 2007; Conduit and Raff, 2010; Jakobsen et al., 2011). However, the molecular mechanisms underlying centrosome asymmetry and its function are incompletely understood (reviewed in Roubinet and Cabernard, 2014).

An ideal system for studying centrosome asymmetry in vivo are *Drosophila* neuroblasts, the neural stem cells of the fly (Homem and Knoblich, 2012; Brand and Livesey, 2011). Neuroblasts establish and maintain centrosome asymmetry during interphase (Januschke et al., 2011, 2013; Conduit and Raff, 2010; Singh et al., 2014; Lerit and Rusan, 2013; Rusan and Peifer, 2007). For instance, their centrosomes separate during early interphase into two centrosomes, containing only one centriole each. These centrioles differ in age and molecular composition; the homolog of the human daughter centriole-specific protein Centrobin (Cnb) localizes to the younger daughter centriole but is absent from the older mother centriole (Januschke et al., 2011). Cnb is phosphorylated by Polo kinase (Plk1 in vertebrates), a requirement to maintain an active MTOC, tethering the daughter centriole-containing centrosome to the apical interphase cortex (Januschke et al., 2013). The mother centriole downregulates Polo and MTOC activity, mediated by Pericentrin (PCNT)-like protein (PLP) and Bld10 (Cep135 in vertebrates) (Singh et al., 2014; Lerit and Rusan, 2013). As a consequence of MTOC downregulation, the mother centriole subsequently moves away from the apical cortex and randomly migrates through the cytoplasm (Rebollo et al., 2007; Rusan and Peifer, 2007; Conduit and Raff, 2010). This centrosome asymmetry is maintained until early prophase, when centrosome maturation starts with the reaccumulation of PCM and the formation of a second MTOC on the basal cortex (Conduit and Raff, 2010; Rebollo et al., 2007; Rusan and Peifer, 2007).

Previously, we showed that Bld10/Cep135 is implicated in the establishment of centrosome asymmetry in *Drosophila* neuroblasts (Singh et al., 2014). Mutations in Cep135 have been linked to primary microcephaly (Hussain et al., 2012), an autosomal recessive neurodevelopmental disorder, manifested in small brains and mental retardation (Nigg et al., 2014). Several loci

(MCPH1–12) have been implicated in primary microcephaly, most of which encode for centrosomal proteins (Nigg et al., 2014). To test whether a causal relationship between centrosome asymmetry and microcephaly exists, we set out to study CG7337, an uncharacterized fly gene corresponding to WD40 repeat protein 62 (WDR62/MCPH2) in vertebrates (Nicholas et al., 2010; Megraw et al., 2011). Mutations in *wdr62* are the second most prevalent cause for microcephaly, but its role in this neurodevelopmental disorder is incompletely understood. WDR62 localizes to the nucleus (Bilgüvar et al., 2010) but also to the spindle poles (Nicholas et al., 2010; Yu et al., 2010; Chen et al., 2014), and it has been implicated in spindle formation and neuronal progenitor cell (NPC) proliferation (Nicholas et al., 2010; Bilgüvar et al., 2010; Yu et al., 2010). WDR62 is a c-Jun N-terminal kinase (JNK) scaffold protein (Wasserman et al., 2010; Cohen-Katsenelson et al., 2011), reported to regulate rat neurogenesis through JNK1 by controlling symmetric and asymmetric NPC divisions in the rat neocortex (Xu et al., 2014). In mice, WDR62 interacts with Aurora A kinase, necessary to regulate spindle formation, mitotic progression, and brain size (Chen et al., 2014). However, whether WDR62 is implicated in other important cellular processes is currently unclear.

Here, we report that CG7337/Wdr62 is required to maintain centrosome asymmetry in *Drosophila* neuroblasts by directly or indirectly stabilizing the interphase MTs necessary to accumulate and maintain PCM-associated Polo. Failure to maintain centrosome asymmetry in *wdr62* mutants perturbs centrosome positioning and segregation as well as spindle orientation. Additionally, and independent of this function, we found that *wdr62* mutant neuroblasts show cell-cycle defects, resulting in a developmental delay and a dramatic reduction in fly brains. We conclude that Wdr62 controls at least two distinct but important aspects of fly neurogenesis.

RESULTS

CG7337, the Fly Ortholog of Wdr62, Is Required to Maintain Centrosome Asymmetry during Interphase

The fly ortholog of Wdr62 is encoded by the uncharacterized gene CG7337 (Megraw et al., 2011; Nicholas et al., 2010), containing several isoforms (Figure S1A), with the longest producing a protein of predicted 2,397 amino acids. Human WDR62 shares, overall, 35% amino acid identity with this CG7337 isoform, and the N terminus alone is 48% identical. Both CG7337 and WDR62 contain three WD40-repeat-containing domains with equal numbers of WD40 repeats (Figure 1A). Due to this conservation and the similarity in domain architecture, we refer to CG7337 as Wdr62 hereinafter.

To assess the function of Wdr62 in the neuroblast centrosome cycle, we generated molecularly defined excision alleles and CRISPR/Cas9 deletions (Experimental Procedures; Figure S1A). The phenotype described in the following sections has been obtained with both the $wdr62^{\Delta 2a}$ and $wdr62^{\Delta 3-9}$ alleles ($wdr62^{\Delta 2a}$/*Df(2L)Exel8005* and $wdr62^{\Delta 3-9}$/*Df(2L)Exel8005*, respectively); both alleles show an identical phenotype, although the phenotypic penetrance is higher with the $wdr62^{\Delta 3-9}$ allele (Figures S1A–S1C). Therefore, unless otherwise noted, we collectively refer hereinafter to either allelic combination as *wdr62* mutant (see figure legends for details on allelic combinations used).

We performed live cell imaging experiments, using DSas4::GFP (Peel et al., 2007) as a centriolar marker in conjunction with the MTOC marker Cherry::Jupiter (Cabernard and Doe, 2009) (Jupiter encodes an MT-binding protein; Karpova et al., 2006). As previously reported (Januschke et al., 2011, 2013; Conduit and Raff, 2010; Singh et al., 2014; Lerit and Rusan, 2013; Rusan and Peifer, 2007), we confirmed that the apical daughter centriole-containing centrosome retained a robust MTOC throughout interphase. The basal mother centriole-containing centrosome, on the other hand, downregulated MTOC activity, preventing the inactive centriole from staying stably anchored at the apical cortex (Figure 1B; Movie S1). *wdr62* mutant centrosomes showed normal DSas4 localization and initially also contained an apical active MTOC. As in wild-type, MTOC activity is normally downregulated on the separating centriole. However, in contrast to wild-type, *wdr62* mutants downregulated MTOC activity on the apical centrosome, on average, within ~30 min, giving rise to two "naked" centrioles, devoid of MTs (Figures 1C, 1F, and 1G; Movie S2). As in wild-type, *wdr62* mutant neuroblasts initiated centrosome maturation in prophase, assembled bipolar spindles, and divided asymmetrically. Nevertheless, they displayed weaker MT intensity on maturing centrosomes and metaphase spindles (Figure 1G). The centrosome asymmetry phenotype of *wdr62* could be rescued by expressing the longest CG7337 isoform with the neuroblast-specific *worniuGal4* (*worGal4*; Albertson and Doe, 2003) driver line, suggesting that this phenotype is neuroblast intrinsic and due to loss of *wdr62* specifically (Figure S1B).

The *wdr62* mutant phenotype is very similar to both *partner of inscuteable* (*pins*; LGN/AGS3 in vertebrates) and *cnb* mutants (Rebollo et al., 2007; Januschke et al., 2013). Cnb and Pins localization was not compromised in *wdr62* mutants. However, the centrosome asymmetry phenotype of neither *pins* nor *cnb* could be rescued with our functional *wdr62* transgene (data not shown). Taken together, these results demonstrate that apical centrosomes devoid of Wdr62 behave like basal wild-type centrosomes and that Wdr62 is required to maintain centrosome asymmetry during interphase.

Wdr62 Is Required to Maintain PCM Proteins on the Apical Interphase Centrosome

Wild-type neuroblasts downregulate basal MTOC activity by shedding PCM proteins such as γ-tubulin (γ-Tub) and centrosomin (Cnn; Cdk5rap2 in vertebrates) (Singh et al., 2014; Conduit and Raff, 2010). We imaged *wdr62* mutant neuroblasts expressing γ-Tub or Cnn in conjunction with the MTOC marker Cherry::Jupiter to test whether the loss of apical MTOC activity is due to PCM protein downregulation. Wild-type neuroblasts retained γ-Tub and Cnn on the apical centrosome throughout interphase (Figure 1D; Movie S3) but *wdr62* mutant neuroblasts lost γ-Tub and Cnn significantly from the apical, daughter centriole-containing centrosome, coincident with the loss of MTOC activity (Figures 1E, 1H, and 1I; Movie S4; data not shown). Consistent with our live-imaging results, we found that fixed *wdr62* mutant interphase neuroblasts contained centrioles with no γ-Tub, whereas all interphase wild-type neuroblast centrosomes were

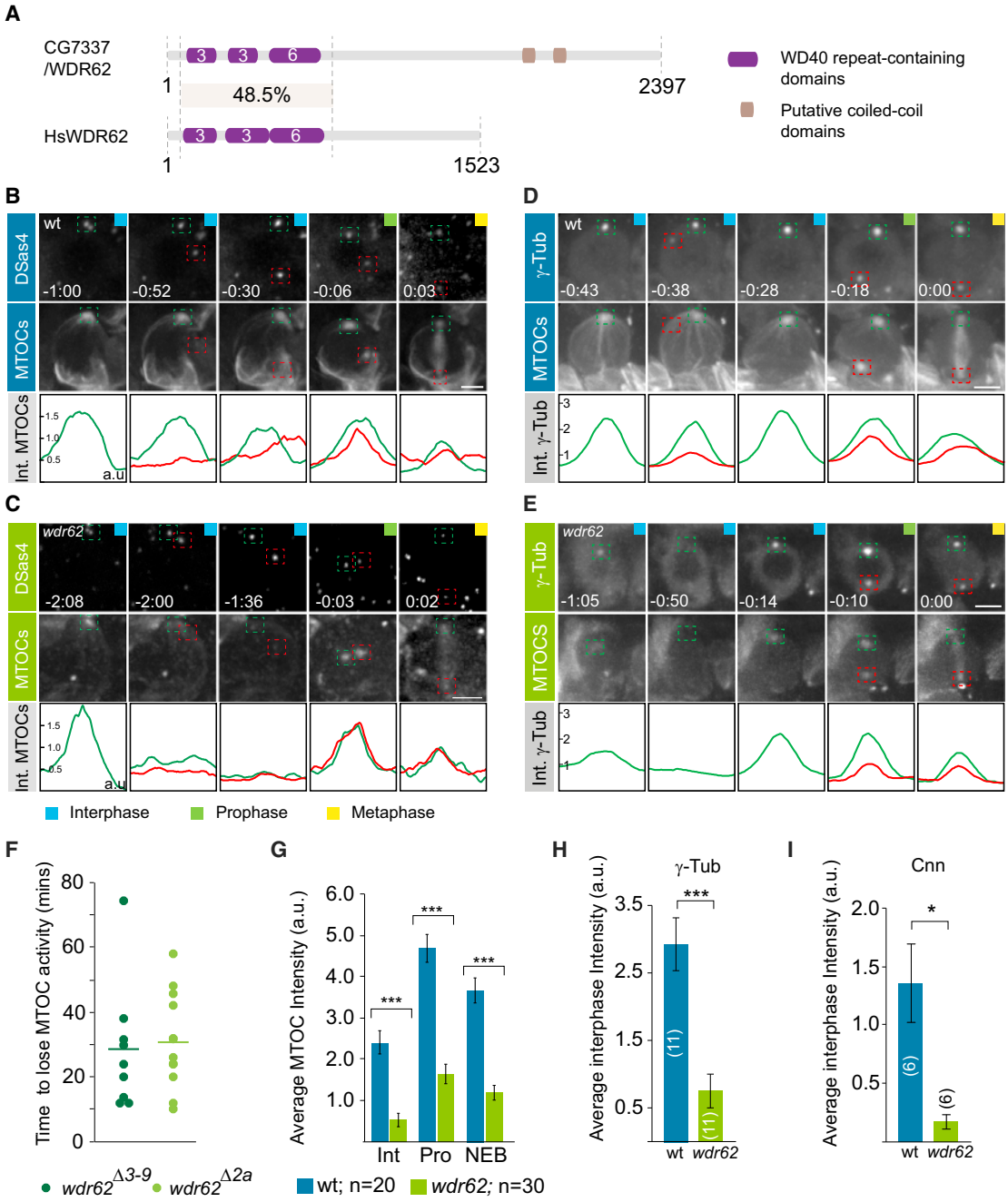

Figure 1. CG7337, the Fly Ortholog of WDR62, Is Required to Maintain Centrosome Asymmetry during Interphase

(A) Domain organization of CG7337 and human WDR62.

(B and C) Wild-type (wt) (B) and *wdr62* mutant (*wdr62*$^{\Delta 2a}$/*Df(2L)Exel8005*) (C) third instar larval neuroblast, expressing the centriolar marker DSas4::GFP (top row) and the MTOC marker Cherry::Jupiter (middle row). For this and subsequent panels, the green and red lines below the image sequence represent intensity (Int.) values of the indicated marker for the apical (green box) and basal (red box) centrosomes, respectively.

(D and E) Wild-type (wt) (D) and *wdr62* (*wdr62*$^{\Delta 2a}$/*Df(2L)Exel8005*) (E) mutant third instar larval neuroblast, expressing the PCM marker γ-Tub::GFP (top row) and the MTOC marker Cherry::Jupiter (middle row).

(F) Quantification of apical MTOC downregulation time in *wdr62* mutants (light green dots indicate *wdr62*$^{\Delta 2a}$/*Df(2L)Exel8005*; dark green dots indicate *wdr62*$^{\Delta 3-9}$/*Df(2L)Exel8005*). The average times are denoted with horizontal green lines.

(G) Cherry::Jupiter intensity measurements at interphase (Int), prophase (Pro), and nuclear envelope breakdown (NEB).

(H and I) Bar graphs representing average intensities for γ-Tub::GFP (H) and Cnn::mCherry (I) during interphase (20 min before NEB). Numbers in bar graphs refer to the number of scored neuroblasts ("ns"). Colored boxes refer to the corresponding cell-cycle stage.

Error bars correspond to SEM. *p < 0.05; ***p < 0.0001. Time is in hours:minutes. Scale bar, 5 μm.

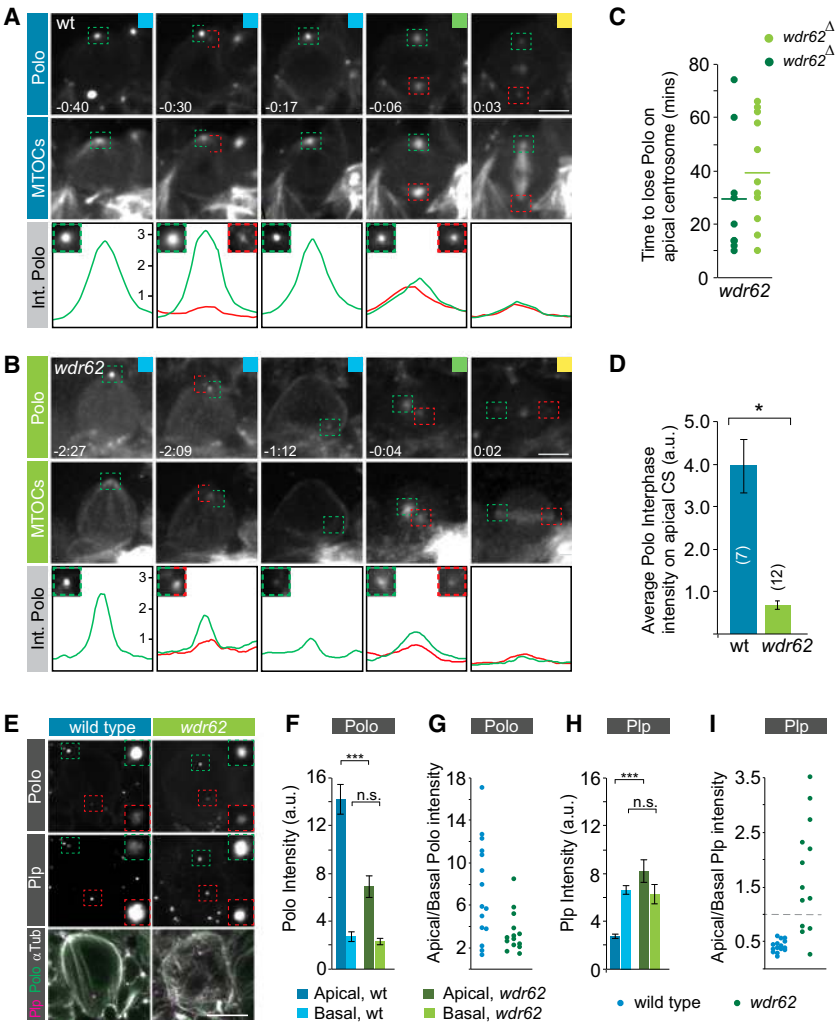

Figure 2. Wdr62 Is Required to Maintain Polo Kinase on the Apical Interphase MTOC

(A and B) Wild-type (wt) (A) and *wdr62* (*wdr62*$^{\Delta 2a}$/*Df(2L)Exel8005*) (B) mutant third instar larval neuroblasts, expressing Polo::GFP (top row) and the MTOC marker Cherry::Jupiter (middle row). The green and red lines below the image sequences represent Polo::GFP intensity (Int.) values of the apical (green box) and basal (red box) centrosomes, respectively.

(C) Quantification of Polo downregulation time in *wdr62* mutants (light green dots indicate *wdr62*$^{\Delta 2a}$/*Df(2L)Exel8005*; dark green dots indicate *wdr62*$^{\Delta 3\text{-}9}$/*Df(2L)Exel8005*). Average times are denoted with horizontal green lines.

(D) Average Polo::GFP intensity during interphase for wild-type (blue bar) and *wdr62* (green bar; *wdr62*$^{\Delta 2a}$/*Df(2L)Exel8005*) mutants.

(E) Representative confocal images of wild-type and *wdr62* mutant (*wdr62*$^{\Delta 3\text{-}9}$/*Df(2L)Exel8005*) neuroblasts stained for Polo (white in single channel and green in overlay), Plp (white in single channel and magenta in overlay), and α-tubulin (white in overlay). Green and red dashed boxes denote the apical and basal centrosomes, respectively, highlighted in the inserts. Contrast and brightness have been adjusted for better visibility.

(F–I) Polo (F) and Plp (H) intensity measurements performed on apical and basal centrosomes in wild-type (dark blue and light blue bars, respectively) and *wdr62* mutant (*wdr62*$^{\Delta 3\text{-}9}$/*Df(2L)Exel8005*; dark green and light green bars, respectively) neuroblasts. Polo (G) and Plp (I) asymmetry ratio for wild-type (blue dots) and *wdr62* mutants (*wdr62*$^{\Delta 3\text{-}9}$/*Df(2L)Exel8005;* green dots). Colored boxes refer to the corresponding cell-cycle stage.

Error bars correspond to the SEM. *$p < 0.05$; ***$p < 0.0001$. Time is in hours:minutes. Scale bars, 5 μm.

asymmetric (Figures S1D and S1E). These data suggest that loss of MTOC activity in *wdr62* mutants is due to downregulation of the PCM proteins γ-Tub and Cnn on the apical centrosome.

Wdr62 Is Required to Maintain Polo Kinase on the Apical Interphase MTOC

Maintenance of MTOC activity during interphase requires Polo kinase (Plk1 in vertebrates) (Januschke et al., 2013; Singh et al., 2014). We used a protein trap line, which endogenously labels Polo with GFP (Buszczak et al., 2007) to image Polo localization in *wdr62* mutants. Wild-type neuroblasts maintained high levels of Polo on the apical MTOC during interphase, whereas basal centrosomes downregulated Polo shortly after centrosome separation (Singh et al., 2014) (Figure 2A; Figure S4B; Movie S5). *wdr62* mutant neuroblasts downregulated Polo as early as 10 min after centrosome separation and contained significantly reduced Polo levels on both interphase centrosomes (Figures 2B–2D; Movie S6). These findings were confirmed in fixed preparations imaged with confocal microscopy (Figures 2E and 2F). The apical centrosome can still be identified because, in most cases, Polo levels are reduced, but not completely absent, resulting in a reduced asymmetry ratio between the apical and basal MTOCs (Figures 2E and 2G). Polo is required for MTOC maintenance, since neuroblasts mutant for the hypomorphic *polo1* allele failed to maintain an active apical MTOC, generating two naked centrioles shortly after centrosomes separated (Januschke and Gonzalez, 2010) (Movie S7; data not shown).

How Polo localization is controlled during interphase is currently not known, but it has been proposed that Plp is involved in the downregulation of Polo on the basal mother centriole. In interphase wild-type neuroblasts, Plp is asymmetrically localized, with the basal centrosome containing more Plp than the apical centrosome (Lerit and Rusan, 2013; Singh et al., 2014). Plp levels are roughly two times higher on the basal than on the apical wild-type centrosome, resulting in a clear asymmetry ratio. In *wdr62* mutants, this ratio was reversed because Plp levels were higher on the apical, Polo-positive centrosome compared to the basal centrosome. In comparison to wild-type apical centrosomes, Plp levels were significantly increased, whereas basal levels did not change significantly (Figures 2E, 2H, and 2I). These data suggest that Wdr62 is required

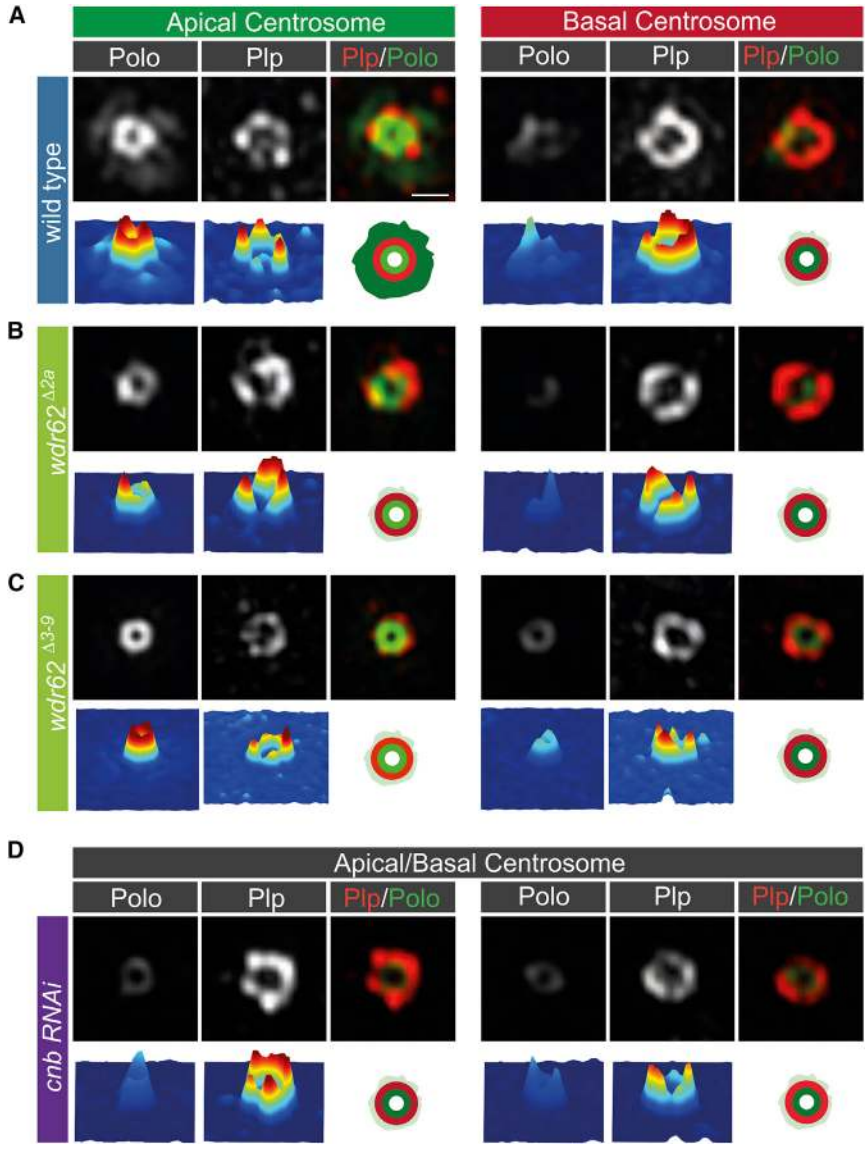

Figure 3. Polo Is Localized to the Centriole and the PCM; Centriolar Localization Depends on Cnb, Whereas PCM Polo Requires Both Wdr62 and Cnb

(A–D) 3D-SIM pictures of representative apical and basal interphase centrosomes in (A) wild-type, (B) *wdr62*$^{\Delta 2a}$, (C) *wdr62*$^{\Delta 3-9}$, and (D) *cnb* RNAi background, labeled with Polo (green in overlay) and Plp (red in overlay). 3D intensity plots are shown underneath the images. A schematic cartoon, summarizing the phenotype, is shown next to the intensity graphs. Since Polo levels were almost equal on both centrosomes in *cnb* RNAi-treated neuroblasts, we cannot clearly distinguish between apical and basal centrosomes. Scale bar, 0.3 μm.

to maintain Polo on the apical centrosome to retain MTOC activity during interphase. Furthermore, it shows that Wdr62 negatively regulates Plp levels on the apical centrosome.

Interphase Centrosomes Contain Centriolar and PCM-Associated Polo

To gain better insight into the relationship of Polo and Plp, we used three-dimensional structured illumination microscopy (3D-SIM; see Experimental Procedures). Using the aforementioned Polo::GFP protein trap line (Buszczak et al., 2007), as well as a previously published Polo::GFP transgene (Moutinho-Santos et al., 1999), we found that the apical, daughter centriole-containing wild-type neuroblast centrosome showed a bright ring of centriolar Polo surrounded by Plp. A diffuse cloud of Polo was localized outside of this irregularly shaped Plp ring. This outer Polo cloud partially overlaps with the PCM marker Cnn, suggesting that Polo extends into the PCM (Figure 3A; Figures S2A and S2B). This finding is consistent with previous reports, showing that Polo also extends into the PCM space in *Drosophila* metaphase S2 cells (Fu and Glover, 2012) and *Drosophila* embryonic interphase centrosomes (Lerit et al., 2015). Basal wild-type neuroblast centrosomes contained almost no PCM-associated and also less centriolar Polo compared to the apical centrosome (Figure 3A). Apical centrosomes in *wdr62* mutants still harbored centriolar Polo surrounded by Plp, but PCM-Polo was no longer detectable. Similarly, basal centrosomes in *wdr62* mutants only contained centriolar Polo, comparable to wild-type neuroblasts (Figures 3B and 3C). In neuroblasts deficient for *cnb*, centriolar Polo was reduced and PCM-Polo was virtually absent; Plp showed a similar arrangement as in wild-type (Figure 3D).

Consistent with our confocal dataset, 3D-SIM imaging also showed that apical wild-type centrosomes contained less Plp than basal wild-type centrosomes, but this was often reversed in *wdr62* mutant neuroblasts (Figures 3A–3C). Since Polo levels are almost equal on both centrosomes in *cnb* RNAi-treated neuroblasts, it is difficult to distinguish between the apical and basal centrosomes. Nevertheless, we found neuroblasts containing both symmetric and asymmetric Plp levels (Figure 3D).

These localization data prompted us to test for molecular interactions between Wdr62, Cnb, Polo, and Plp. We performed a yeast-two hybrid assay and found an interaction between Cnb and Plp but not between Wdr62, Plp, and Polo (Figure S2C). Taken together, these results demonstrate that loss of Wdr62 or Cnb perturbs the asymmetric localization of Polo and Plp. Furthermore, it shows that the PCM-associated Polo fraction on the apical centrosome is regulated by Wdr62 and Cnb. Cnb also controls the centriolar Polo pool on the apical centrosome.

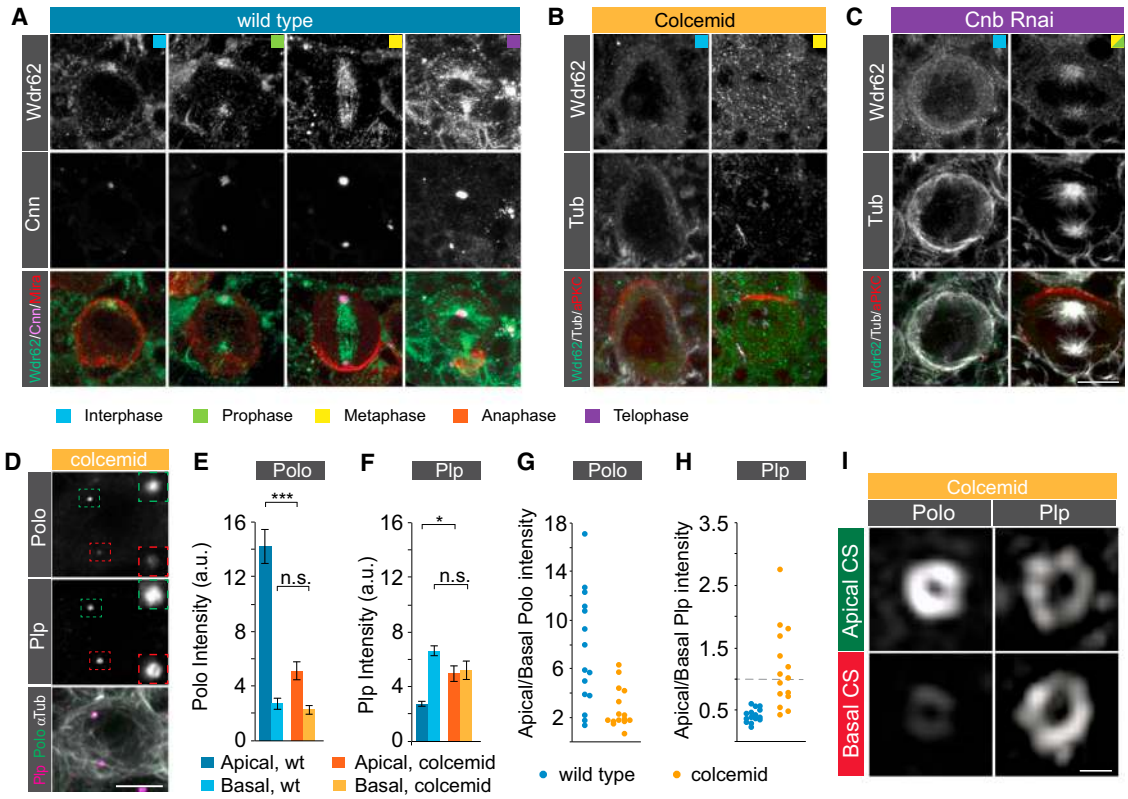

Figure 4. Wdr62 Is a MT-Associated Protein, Controlling PCM Polo through Stabilization of MTs

(A) Representative wild-type neuroblast stained with the Wdr62 peptide antibody (green in overlay), the PCM marker Cnn (magenta in overlay), and the neuroblast marker Miranda (Mira; red in overlay).

(B and C) Colcemid-treated wild-type (B) and *cnb* RNAi (C) neuroblasts stained for Wdr62 (green in overlay), the spindle marker α-tubulin (white in overlay), and the apical polarity marker atypical protein kinase C (aPKC) (red in overlay).

(D) Representative confocal neuroblast pictures showing Polo (white in single channel and green in overlay), Plp (white in single channel and magenta in overlay) and α-tubulin (white in overlay) after colcemid treatment. Green and red dashed boxes denote the apical and basal centrosomes, respectively, highlighted in the inserts. Contrast and brightness has been adjusted for better visibility.

(E and F) Polo (E) and Plp (F) intensity measurements performed on apical and basal centrosomes in wild-type (wt) (dark blue and light blue bars, respectively) and colcemid-treated wild-type neuroblasts (dark orange and light orange bars, respectively).

(G and H) Polo (G) and Plp (H) asymmetry ratio for wild-type (blue dots) and colcemid-treated wild-type neuroblasts (orange dots).

(I) Representative 3D-SIM centrosome pictures of Polo and Plp after colcemid treatment. Colored boxes refer to the corresponding cell-cycle stage.

Error bars correspond to SEM. *$p < 0.05$; **$p < 0.001$; ***$p < 0.0001$; n.s; not significant. Time is given in hours:minutes. Scale bars, 5 μm in (C) and (D) and 0.3 μm in (I).

Wdr62 Is a Spindle-Associated Protein and Depends on MTs for Its Localization

To get further mechanistic insight into Wdr62's role in centrosome asymmetry, we analyzed its localization in third instar larval neuroblasts using three different reagents: (1) a functional *wdr62::mDendra2* transgene (Figures S1B and S3A); (2) a protein trap line, tagging all *wdr62* isoforms (Figures S3B and S3C); and (3) two peptide antibodies, recognizing two distinct Wdr62 antigens (Figure 4A; Figure S3D). All reagents showed comparable results; Wdr62 was localized on the apical, active MTOC during interphase. From prophase onward, Wdr62 also became enriched on the maturing basal centrosome and subsequently decorated the spindle from metaphase throughout mitosis. Wdr62 did not completely overlap with canonical PCM markers such as Cnn but suggested an association with MTs instead (Figure 4A). Indeed, chemical spindle ablation experiments using colcemid resulted in diffuse cytoplasmic Wdr62 localization when MTs were absent (Figure 4B). Similarly, removal of the interphase MTOC by knocking down *cnb* resulted in mostly cytoplasmic Wdr62 localization; Wdr62 relocalized to the spindle during prophase and metaphase (Figure 4C). These data provide evidence that Wdr62 is an MT-associated protein and is asymmetrically localized during interphase.

PCM-Associated Polo Localization Depends on Intact MTs

Wdr62's spindle association prompted us to test whether centrosomal Polo levels could also be directly regulated through MTs. To this end, we depolymerized MTs using colcemid and analyzed the localization of Polo and Plp in interphase neuroblasts with confocal microscopy. Colcemid treatment resulted in a significant drop in apical Polo levels and close to a 2-fold

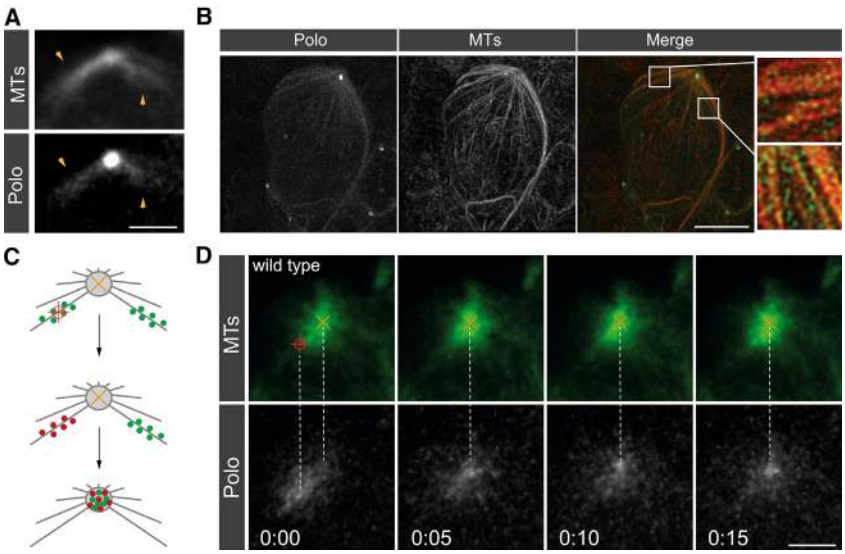

Figure 5. Polo Is Localized on MTs and Travels to the Centrosome

(A) Representative live-imaging snapshots of a late-telophase wild-type neuroblast expressing Cherry::Jupiter (MTs; top row) and Polo::GFP (protein trap line; bottom row). Yellow arrowheads denote MT fibers decorated with Polo.

(B) 3D-SIM pictures of an interphase wild-type neuroblast expressing Polo::GFP (protein trap line; green in overlay) and stained for α-tubulin (MTs; red in overlay). Higher magnifications of two selected regions are shown in high-magnification inserts.

(C) Cartoon illustrating photoactivation experiments for wild-type neuroblasts.

(D) Representative image sequence of a wild-type neuroblast expressing the MT marker G147 (MTs; top row; green) and Polo::mDendra2 (photoconverted in bottom row [white]). Red crosshairs represent the target area, which was photoconverted. Yellow crosses represent the center of the centrosome. Time is given in hours:minutes.

Scale bars, 5 μm.

increase of Plp on the apical interphase centrosome. Basal Polo and Plp did not change significantly upon colcemid treatment (Figures 2E and 4D–4F). As a consequence of decreased apical Polo levels, the apical/basal asymmetry ratio dropped to a level comparable to that of *wdr62* mutants (Figures 2G and 4G). Similarly, Plp asymmetry ratios were often inverted (Figures 2I and 4H).

To further asses the dynamics of Polo localization in interphase when MTs are partially depolymerized or absent, we applied low doses of colcemid to *zeste-white 10* (*zw10*) mutant neuroblasts and followed the behavior of endogenously tagged Polo (Polo::GFP) and Cnn (Cnn::mCherry), as well as MTs with live cell imaging. *zw10* mutants lack the spindle assembly checkpoint, permitting neuroblasts to enter anaphase when the mitotic spindle is missing (Basto et al., 2000). We found that a low dose of colcemid was mimicking the *wdr62* mutant phenotype; interphase MTs were depolymerized, but centrosome maturation and bipolar spindle formation were not inhibited in metaphase (Figures S4A, S5A and S5B; 100%, n = 70). In contrast to *zeste-white 10* control neuroblasts, Polo levels dropped on the apical interphase centrosome as MTs were depolymerized (100%, n = 40). The localization of Cnn was dependent on Polo; a colcemid-induced reduction in Polo was accompanied by a drop in Cnn levels (Figures S4A–S4C and S5B; 100%, n = 40). Furthermore, in *zw10* control neuroblasts, Cnn was shed on the basal centrosome shortly after Polo had been down-regulated (Figure S4B; time point, −0:38) and reappeared after Polo relocalized on the maturing basal centrosome (Figure S4B; time point, −0:08). However, the apical centrosome always retained Polo, Cnn, and MTOC activity in *zw10* mutant neuroblasts that have not been exposed to colcemid (Figures S4B and S5A; 100%, n = 67).

Finally, we also confirmed with 3D-SIM that PCM-Polo was absent from the apical interphase centrosome upon colcemid treatment. Centriolar Polo was not affected, and the lack of MTs did not seem to change the localization pattern of Plp (Figure 4I).

Collectively, these results suggest that MTs are required for the recruitment and/or maintenance of Polo on the apical centrosome. It also shows that maintenance of Cnn on the active interphase centrosome and accumulation during maturation both depend on Polo. Furthermore, these data show that MTs regulate PCM-associated Polo and Plp levels. Importantly, depletion of *wdr62* and loss of MTs show very similar phenotypes.

Astral MTs Recruit Polo to the Apical Interphase Centrosome

To test whether MTs recruit Polo to the apical centrosome, we first checked whether Polo colocalizes with MTs. Indeed, our live imaging data showed that Polo overlaps with astral MTs, predominantly during late telophase and in interphase (Figure 5A). Furthermore, 3D-SIM imaging of the Polo::GFP protein trap line (Buszczak et al., 2007) or a Polo::GFP transgene (Moutinho-Santos et al., 1999) shows Polo decorating MTs in interphase neuroblasts (Figure 5B and data not shown).

To confirm that MTs actively recruit Polo to the centrosome, we devised an in vivo pulse-chase experiment. To this end, we generated transgenic flies expressing Polo fused to the photoconvertable fluorescent protein mDendra2, expressed under the control of Polo's endogenous regulatory elements (see Experimental Procedures; Moutinho-Santos et al., 1999). We crossed Polo::mDendra2 to G147, a protein trap line labeling the MT-binding protein Jupiter with GFP endogenously (Morin et al., 2001; Karpova et al., 2006), and photoconverted Polo::mDendra2 on astral MTs ~4–7 μm away from the centrosome. If Polo travels on MTs to the centrosome, then photoconverted Polo::mDendra2 on MTs should relocalize to the center of the apical centrosome (Figure 5C). We performed this experiment in interphase wild-type neuroblasts and observed in all cases (100%; n = 10) that Polo relocalized from the periphery of the MTOC to the centrosome center (Figure 5D). Furthermore, if Polo::mDendra2 is photoconverted in the cytoplasm or colcemid-treated neuroblasts, showing a reduction, albeit not a complete lack, of astral MTs, relocalization of photoconverted

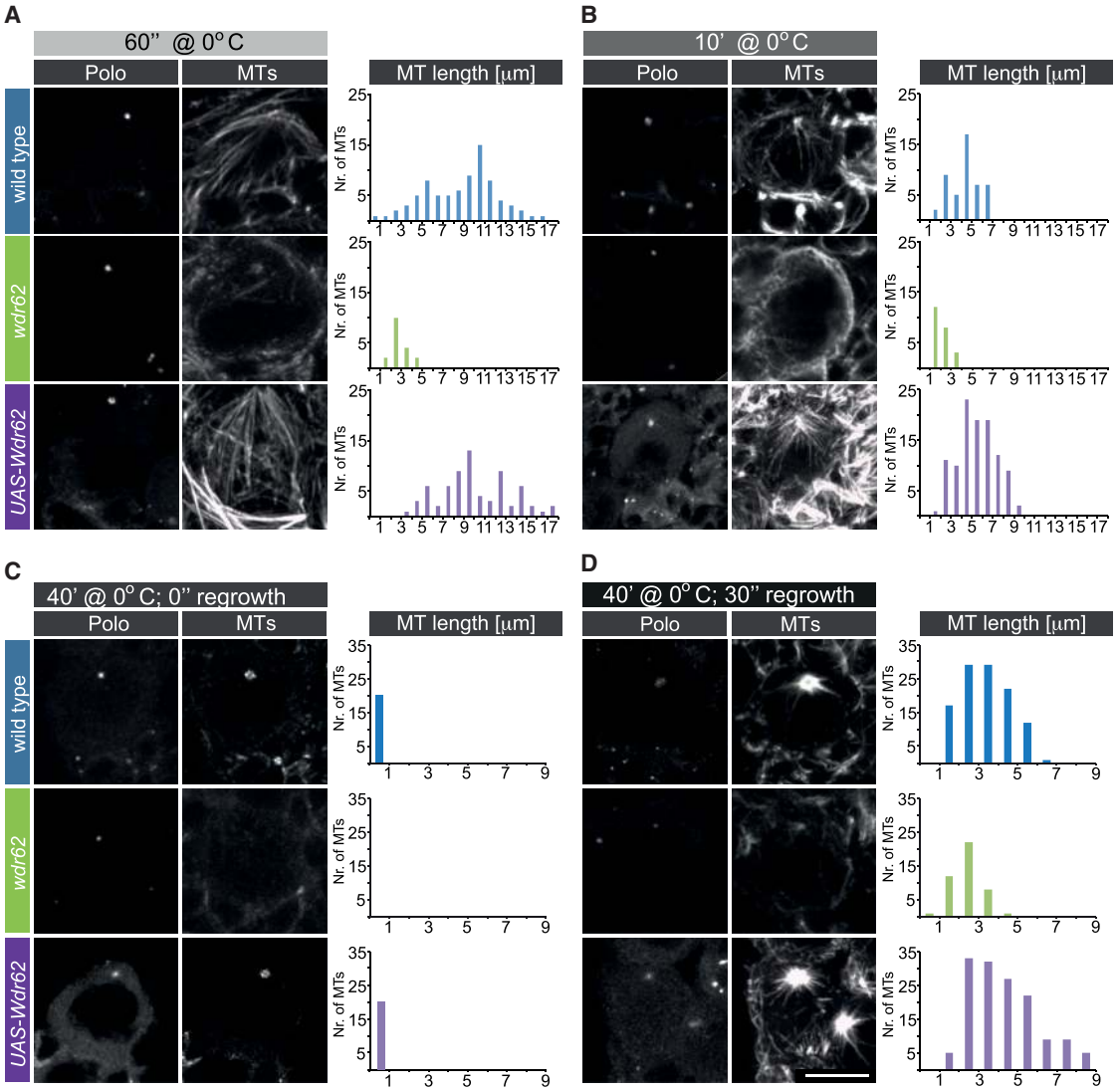

Figure 6. Wdr62 Is Stabilizing MTs

(A–D) Representative confocal images of wild-type (top row), *wdr62* mutant (*wdr62*$^{43\text{-}9}$/*Df(2L)Exel8005*), or Wdr62-overexpressing (*UAS-Wdr62:mDendra2*) neuroblasts incubated at 0°C for (A) 60 s, (B) 10 min, (C) 40 min, or (D) 40 min, followed by 30 s regrowth at room temperature. In all genotypes, neuroblasts co-expressed Polo::GFP and were stained for α-tubulin. Bar graphs represent quantifications of MT bundle length for the indicated conditions. Nr, number. Scale bar, 5 μm.

Polo::mDendra2 to the centrosome was barely detectable (100%; n = 5; Figures S6A–S6D).

These results demonstrate that Polo is localized to astral MTs in interphase neuroblasts and is actively being recruited to the apical centrosome. Although, at this level of resolution, we cannot determine whether Polo will be recruited to the PCM or the centriole, the structure of the centrosome predicts that photoconverted Polo will first become enriched in the PCM. Collectively, these data provide strong evidence that MTs are required to recruit Polo to the apical interphase centrosome.

Wdr62 Stabilizes Interphase MTs

Since *wdr62* mutants and depletion of MTs show a similar phenotype, and Wdr62 is localized to MTs, we next wanted to test the hypothesis whether Wdr62 is required to stabilize interphase MTs. MTs can dynamically switch between growth and shrinkage (catastrophe), modulated by many MT-associated proteins (MAPs) (Godek et al., 2015). We applied a cold assay to test whether the lack of, or excess of, Wdr62 would alter this dynamic instability in *Drosophila* neuroblasts. Incubating neuroblasts at 0°C will induce MTs to depolymerize. For instance, increasing the incubation time on ice from 60 s to 10 min increases the number of short interphase MTs for wild-type, *wdr62* mutants, and neuroblasts overexpressing Wdr62 (UAS-Wdr62::mDendra2). This effect was strongest in *wdr62* mutants, whereas Wdr62-overexpressing cells were affected the least (Figures 6A and 6B). If neuroblasts are incubated on ice for 40 min, MTs are almost completely

depolymerized; wild-type and Wdr62-overexpressing cells only contain a tubulin ring, surrounding Polo. However, cells lacking Wdr62 completely lost this tubulin ring but retained weak levels of Polo (centriolar Polo, most likely; Figure 6C). To measure MT regrowth, we first incubated wild-type, *wdr62* mutant, and Wdr62-overexpressing cells on ice for 40 min, followed by a temperature shift to 25°C for 30 s. Whereas wild-type neuroblasts can regrow MTs up to 7 μm (with the majority being between 2 and 6 μm in length), overexpressing Wdr62 shifted MT length toward 9 μm. *wdr62* mutant neuroblasts predominantly contained fewer and shorter MT bundles (Figure 6D). Polo intensity usually correlated with MT length and density.

These data show that MTs in *wdr62* mutant neuroblasts are more sensitive to cold than wild-type and that Wdr62-overexpressing cells are less sensitive than wild-type. Furthermore, the amount of Wdr62 protein determines MT regrowth rates, manifested in MT length. Collectively, these data suggest that Wdr62 is required to either directly or indirectly stabilize interphase MTs. Based on these results, we propose that stabilized MTs are required to recruit Polo to the apical interphase centrosome.

Wdr62 Affects Centrosome Positioning, Spindle Orientation, and Centrosome Segregation

Defects in centrosome asymmetry have been shown to compromise centrosome positioning, spindle orientation, and centrosome segregation (Januschke et al., 2013; Januschke and Gonzalez, 2010; Lerit and Rusan, 2013; Singh et al., 2014), and we tested whether *wdr62* mutants show similar phenotypes. To this end, we first tracked centrioles during interphase until prophase in wild-type and *wdr62* mutant neuroblasts. Consistent with earlier reports (Rebollo et al., 2007; Singh et al., 2014), we found that wild-type apical centrosomes remain tethered to the apical cortex. Basal wild-type centrioles, however, lost their apical position, wandering randomly through the cytoplasm. In *wdr62* mutant neuroblasts, the apical centrosome was no longer stationary; both track length and overall centrosome displacement were similar between the apical and basal centrioles and significantly increased compared to wild-type centrioles (Figures 7A and 7B).

Centriole displacement compromises the correct positioning of centrosomes shortly before bipolar spindle formation. We measured centrosome position at prophase in relation to the metaphase spindle axis and confirmed that, in wild-type neuroblasts, the apical centrosome stayed close to the apical cortex throughout interphase. The basal centrosome, on the other hand, started maturing close to the basal cortex (Figure 7C; Singh et al., 2014). In *wdr62* mutants, apical centrosomes showed a more widespread distribution and matured close to the basal cortex in several instances (Figure 7D).

Centrosome displacement can also affect spindle orientation, and we tested this in fixed preparations by measuring the orientation of the mitotic spindle in relation to the neuroblast intrinsic polarity axis. Indeed, in contrast to wild-type, *wdr62* mutant neuroblasts contained misaligned spindles with low frequencies (Figures 7E and 7F). However, live cell imaging experiments demonstrated that misaligned spindles realigned with the neuroblast intrinsic apical-basal polarity axis (Figure 7G). This realignment often failed to correctly reposition centrosomes, which manifested in centrosome segregation defects. Wild-type neuroblasts retained the younger daughter centriole-containing centrosome and segregated the older mother centriole into the differentiating ganglion mother cell (GMC) (100%; n = 79) (Conduit and Raff, 2010; Januschke et al., 2011; Singh et al., 2014). In *wdr62* mutants, centriole segregation was mildly compromised; 16% of *wdr62* mutant neuroblasts retained the centrosome containing the older mother centriole (n = 43; Figure 7H). These results are consistent with previous findings, showing that centrosome asymmetry defects can result in centrosome missegregation (Januschke et al., 2013; Singh et al., 2014).

Wdr62 Is Required for Normal Cell-Cycle Progression

Since *wdr62* has been implicated in primary microcephaly (Nicholas et al., 2010; Yu et al., 2010; Bilgüvar et al., 2010), we staged larval brains and performed brain size measurements, analyzing both optic lobe neuroepithelium and central brain size. Interestingly, we found that *wdr62* mutant brains are ~40% smaller compared to wild-type brains (Figures S7A and S7B). The brain size decrease is mostly attributed to a smaller central brain but not a reduction in the optic lobe (data not shown). Central brain size reduction could be a consequence of the observed centrosome asymmetry phenotype. Alternatively, cell-cycle delays, apoptosis, or a depletion of the neural stem cell pool could compromise brain development. To test this, we also knocked down *cnb* but did not find a brain size reduction (Figures S7A and S7B). Also, neuroblast number was only slightly reduced in *wdr62* but not in *cnb* RNAi brains (Figure S7C). However, our cell-cycle measurements showed that, in *wdr62* mutants, the cell cycle is significantly increased, affecting both interphase and mitosis length (Figures S7D and S7E). This neuroblast cell-cycle delay might not be specific to neuroblasts, since *wdr62* mutants are developmentally delayed (data not shown). However, the increase in neuroblast cell-cycle length is uncoupled from *wdr62*'s centrosome asymmetry phenotype since we also found ~50% of neuroblasts in $wdr62^{\Delta 3-9}$ mutants with a cell cycle comparable to that of wild-type neuroblasts, showing loss of apical MTOC activity (Figures S7F and S7G). Since lack of Cnb did not show any cell-cycle delays (Figure S7D), we conclude that the observed brain size reduction is due to an increase in cell-cycle length and an overall developmental delay.

DISCUSSION

Here, we show that CG7337, the fly ortholog of the microcephaly protein MCPH2/WDR62, is required to maintain centrosome asymmetry in *Drosophila* neural stem cells. We demonstrate that Wdr62 is a spindle-associated protein, localizing to the active interphase MTOC and subsequently also decorating the entire mitotic spindle. In agreement with this localization, we demonstrate that Wdr62 is required to directly or indirectly stabilize MTs and to maintain MTOC activity on the apical interphase centrosome. In *wdr62* mutants, Polo, Cnn, and γ-Tub are downregulated, causing a loss in apical MTOC activity. These findings are consistent with previous reports, showing that maintenance of apical MTOC activity in interphase neuroblasts depends on

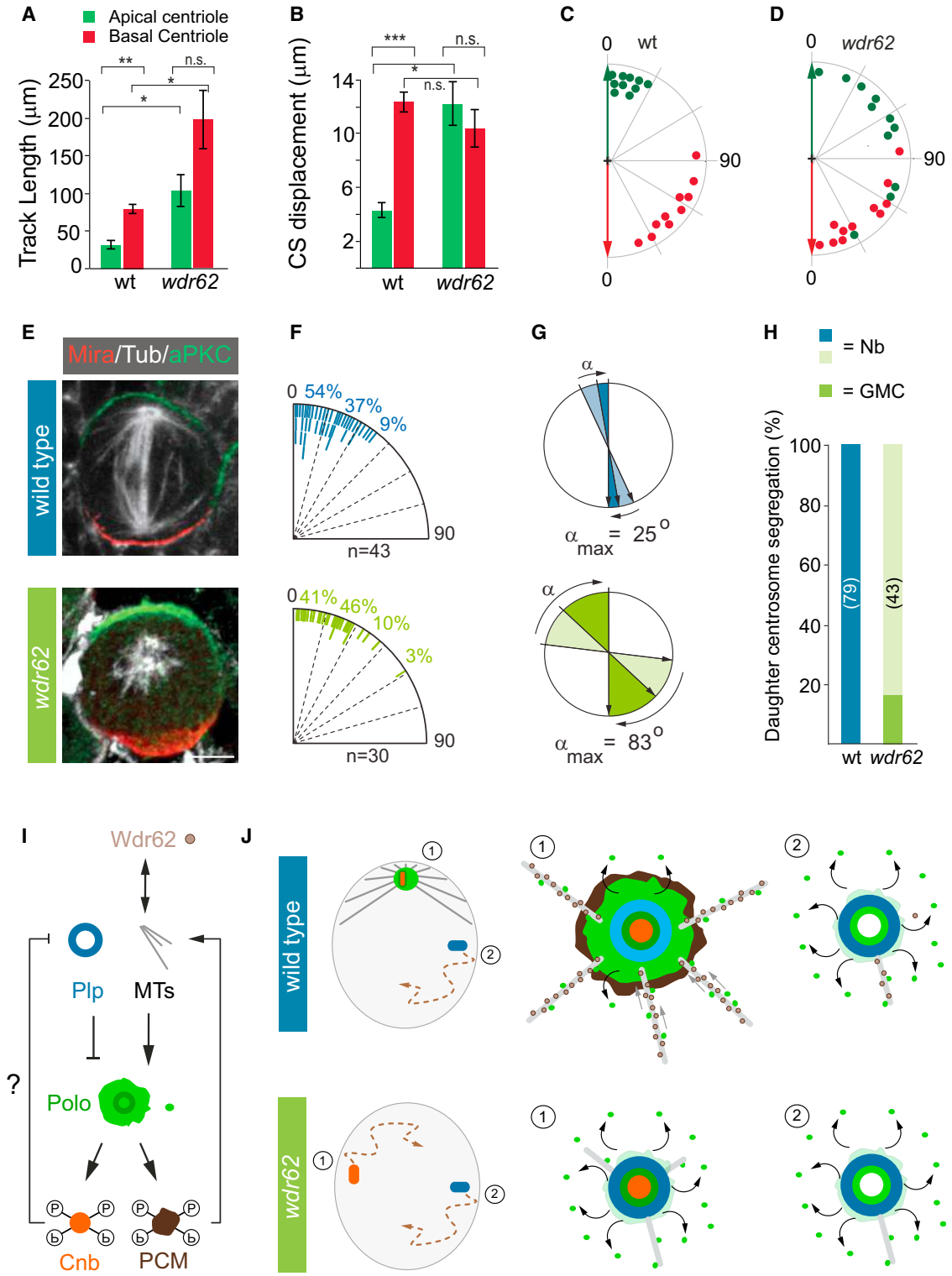

Figure 7. Loss of Wdr62 Compromises Centrosome Positioning, Spindle Orientation, and Biased Centrosome Segregation

(A–D) Mean track length (A) and centrosome (CS) (B) displacement for the apical (green bars) and basal (red bars) centrosomes in wild-type (wt) (n = 7) and *wdr62* mutants (*wdr62*$^{\Delta 2a}$/*Df(2L)Exel8005*; n = 8). Radial centrosome distribution plot of wild-type (C) and *wdr62* (*wdr62*$^{\Delta 2a}$/*Df(2L)Exel8005*) mutants (D) depicting the maximal deviation of the apical (green) and basal (red) prophase MTOC in relation to the metaphase spindle axis ("0" degree line). Green and red arrows highlight the apical (green)/basal (red) polarity and division axis.

(legend continued on next page)

the mitotic kinase Polo/Plk1 (Januschke et al., 2013). Polo has been shown to phosphorylate PCM components such as Cnn (Conduit et al., 2014) but also the daughter centriole-specific protein Cnb, which is necessary to maintain MTOC activity (Januschke et al., 2013). How Polo's localization is controlled is unclear, but in *Drosophila* neuroblasts, it was reported that Polo levels are partially regulated through Plp (Lerit and Rusan, 2013; Singh et al., 2014). Plp is asymmetrically localized in wild-type neuroblasts, containing higher Plp on the mother centriole-containing basal centrosome. This asymmetric localization could be controlled through a direct molecular interaction between Cnb and Plp, since ectopically localizing Cnb to both centrosomes decreases Plp levels (Singh et al., 2014; Lerit and Rusan, 2013), and our yeast-two hybrid data indicate that Cnb directly interacts with Plp. Cnb localization does not change in *wdr62* mutants, but Plp levels increase on the apical centrosome with the consequence that both centrosomes contain similar levels of Plp.

Plp and Polo could also be regulated through other mechanisms. For instance, using 3D-SIM, we further discovered that apical interphase neuroblast centrosomes contain a centriolar and a PCM-associated pool of Polo protein. PCM-associated Polo has recently been seen in metaphase centrosomes of *Drosophila* S2 cells (Fu and Glover, 2012) and embryonic interphase centrosomes (Lerit et al., 2015). *wdr62* specifically perturbed the localization of Polo associated with PCM, whereas Cnb is required to maintain both PCM and centriolar Polo.

Based on our results and previously published data, we propose the following model: neuroblasts exit mitosis with a robust array of MTs, which originates from the preceding centrosome maturation cycle. This array is used to increase the amount of Polo protein on the apical Cnb^{+} centrosome through new recruitment as the neuroblast exits mitosis. Indeed, our live imaging and 3D SIM data show that interphase MTs are decorated with Polo and that colcemid treatment decreases PCM Polo levels. Furthermore, Polo levels are usually lowest at metaphase, increase after mitosis, and stay high throughout interphase. Polo recruitment to the centrosome occurs via astral MTs, which is supported by our photoconversion experiments. To allow for sustained Polo recruitment, we propose that Wdr62 stabilizes interphase MTs, which is consistent with Wdr62's localization, live imaging, and cold assay data. To maintain this cycle, Polo needs to phosphorylate not only PCM proteins (e.g., Cnn; Conduit et al., 2014) but also Cnb (Januschke et al., 2013). This is consistent with previous data, showing that increasing levels of Polo on the basal centrosome transforms the basal centrosome into an active MTOC, failing to shed the Polo target Cnn (Lerit and Rusan, 2013; Singh et al., 2014). Furthermore, *cnb* phosphomutants are unable to rescue *cnb*'s loss-of-function phenotype (Januschke et al., 2013). Our model further proposes that phosphorylated Cnb is necessary to prevent Plp protein levels from increasing on the apical interphase centrosome. Indeed, we found that Cnb directly interacts with Plp. The basal centrosome, however, also recruits Polo through MTs, but due to the lack of Cnb, Plp is upregulated, inducing the shedding of Polo and PCM and preventing the maintenance of MTs and, thus, the new recruitment of Polo (Figures 7I and 7J).

This model predicts that loss of Wdr62 and depletion of MTs should have the same phenotype. In support of this, we found that loss of MTs mimics the phenotype of *wdr62* mutants; in colcemid-treated neuroblasts, Polo and Cnn are downregulated on the apical centrosome with a concomitant increase in Plp, reaching levels similar to that of the basal centrosome. Furthermore, PCM-associated Polo is lost. Taken together, we propose that maintenance of the apical, daughter centriole-containing centrosome's MTOC activity—and, thus, neuroblast centrosome asymmetry—can be established and maintained by balancing Plp-mediated shedding of Polo and MT-dependent Polo recruitment and maintenance. Wdr62 plays a key role in this process by stabilizing MTs.

Similar to *wdr62*, *pins* mutant neuroblasts also show loss in interphase MTOC activity (Rebollo et al., 2007). However, since Pins does not co-localize with Wdr62 and Cnb during the neuroblast cell cycle, it is currently unclear how this protein affects interphase MTOC activity. Pins could compromise Polo localization in interphase in a Cnb- and Wdr62-independent manner. Alternatively, since Pins has been reported to affect spindle asymmetry (Cai et al., 2003), it could also influence centrosome architecture in mitotic neuroblasts, preventing the apical centrosome from maintaining MTOC activity in interphase. Recently, we also implicated Bld10 in Polo and PCM shedding (Singh et al., 2014), but additional work is needed to fit Bld10 and Pins into the proposed model.

MTOC asymmetry is important for proper centrosome positioning and spindle orientation (Januschke et al., 2013; Januschke and Gonzalez, 2010; Lerit and Rusan, 2013; Singh et al., 2014) (Figure 7). Whereas wild-type neuroblasts always retain the daughter centriole-containing centrosome, *wdr62* mutants show centrosome segregation defects with low frequency. Similarly, spindle orientation defects occur but are corrected in *wdr62* mutants, suggesting that backup mechanisms are in place to detect and correct spindle misalignment if centrosome mispositioning occurs (Singh et al., 2014). Our phenotypic analysis also revealed that Wdr62 is involved in normal brain

(E) Representative wild-type and *wdr62* mutant (*wdr62$^{\Delta 2a}$/Df(2L)Exel8005)* neuroblasts stained for the apical marker aPKC (green), the basal marker Miranda (Mira; red) and α-tubulin (white).
(F) Quantification of spindle orientations in fixed neuroblasts. Tick marks (wild-type; blue. *wdr62 (wdr62$^{\Delta 2a}$/Df(2L)Exel8005)*; green) represent the orientation of metaphase spindles with respect to the polarity axis.
(G) Spindle correction angles; wild-type (blue) and *wdr62* (*wdr62$^{\Delta 2a}$/Df(2L)Exel8005;* green). Mean correction angles (α-mean) are shown in darker shading and the maximal correction angle (α-max) is shown in lighter shading. Wild-type: α-max = 24.7°; α-mean = 15° ± 6.8°; n = 10. *wdr62*: α-max = 83°; α-mean: 38° ± 30°; n = 11).
(H) Quantification of centrosome segregation in wild-type (blue bar) and *wdr62* (*wdr62$^{\Delta 2a}$/Df(2L)Exel8005;* green bars) mutant neuroblasts.
(I) Model: Wdr62 (brown balls) is associated with MTs and is stabilizing interphase MTs, permitting the recruitment of Polo to the centrosome.
(J) This mechanism ensures the maintenance of an active apical MTOC in interphase neuroblasts. See Discussion for details.
Error bars indicate SEM. *p < 0.05; **p < 0.001; ***p < 0.0001; n.s., not significant. Scale bar, 5 μm.

development, in agreement with previously published vertebrate model systems (Chen et al., 2014; Xu et al., 2014). Wdr62 mutant brains are ~40% smaller compared to wild-type brains, showing only a minor decrease of neural stem cells. Based on our cell-cycle measurements, the simplest interpretation is that cell-cycle delays cause a reduction in brain size. In embryonic neural stem cells, Wdr62 controls mitotic progression through interactions with Aurora A kinase (Chen et al., 2014), and we hypothesize that the same mechanism could control neuroblast cell-cycle progression, which is consistent with the *aurA* mutant neuroblast phenotype (Lee et al., 2006). Inactivation of the apical MTOC does not seem to compromise normal brain development, since *cnb* RNAi-treated animals show normal cell-cycle length and normal brain size. However, the aforementioned backup mechanisms, correcting centrosome mispositioning and spindle misorientation, could prevent more severe developmental perturbations. This hypothesis is consistent with a recent report showing that centrosome cycle misregulation compromises spindle orientation in mouse neural progenitors, biasing the progenitor division mode toward asymmetric divisions (Gruber et al., 2011).

Although we failed to find a causal relationship between centrosome asymmetry and microcephaly, perturbed centrosome segregation could affect brain development in ways that have escaped our attention so far. For instance, recent reports suggest that biased sister chromatid and midbody segregation could be connected with centrosome asymmetry (Salzmann et al., 2014; Yadlapalli and Yamashita, 2013). Thus, the finding that centrosome positioning and biased centrosome segregation is highly stereotypic would argue for an important function of this process. However, more refined assays will be necessary to determine the consequence of compromised centrosome asymmetry. Taken together, we discovered that Wdr62 is required to stabilize MTs, ensuring MTOC activity and centrosome asymmetry, a requirement for spindle orientation and biased centrosome segregation.

EXPERIMENTAL PROCEDURES

Fly Strains and Genetics

A detailed list of all the generated and used fly strains and transgenes can be found in the Supplemental Experimental Procedures.

Antibodies Used

Mouse anti-Wdr62 (1:1,000) monoclonal peptide antibodies were generated by Abmart for the following epitopes: MTPASLSASTPT (Wdr62(1–12)) and NTENGKSVAAPP (Wdr62(1154–1165)). For the representative images in Figure 5, Wdr62(1–12) was used; Wdr62(1154–1165; 1:1,000) yielded almost identical results. All the other antibodies used in this study can be found in the Supplemental Experimental Procedures.

Immunostainings

At 96–120 hr (AEL; after egg laying), larval brains were dissected and fixed as previously described (Singh et al., 2014). Please refer to the Supplemental Experimental Procedures for details.

Cold Assay for MT Dynamics

Brains (96-hr AEL) were dissected and transferred to 50 μl of Schneider's medium and incubated on ice for 1, 10, or 40 min and either fixed immediately or incubated at 25°C in a water bath for 30 s. Subsequently, brains were fixed and stained with mouse anti-α-Tub (Serotec; 1:1,000) and rabbit anti-Cnn (1:1,000). Complete depolymerization of long MTs was seen in all wild-type interphase neuroblasts after 40 min on ice. MT length was measured in Imaris 7.4 and higher.

Colcemid Treatment

To inhibit MT formation, wild-type brains were dissected in Schneider's medium and incubated for 1 hr with colcemid (Sigma) at a final concentration of 20 μg/ml. Brains were fixed and stained as described earlier. For the Polo::mDendra2 photoconversion experiments, we used imaging media and 20 μg/ml colcemid (final concentration). For live-imaging colcemid experiments, larval brains (96 hr AEL) were dissected in imaging medium and incubated with 5 μg/ml of colcemid (final concentration).

Live Imaging Sample Preparation

Live imaging experiments were performed as previously published (Cabernard and Doe, 2013) and explained in the Supplemental Experimental Procedures.

Photoconversion

Photoconversion experiments were performed on G147 (tagging Jupiter with GFP [Morin et al., 2001; Karpova et al., 2006]) larvae (96 hr AEL), crossed to *polo::mDendra2* (this work; discussed earlier). We used an Andor Revolution spinning disc system equipped with the FRAPPA unit. A regions of interest (ROI) was manually chosen in the GFP channel. MT signal from G147 allowed for unambiguous identification of interphase neuroblast MTs. Astral MTs were irradiated at various distances away from the active centrosome. Before photoconversion, single Z planes containing ROIs were scanned for ten time points with maximum speed. Subsequently, ROIs were irradiated with the 405-nm laser line (~15%; 20 repeats; 50-μs dwell time). After photoconversion, the entire neuroblast was scanned with a z-step size of 0.65 μm. Photoconverted Polo::mDendra2 emits red fluorescence, which was detected simultaneously with G147's GFP emission GFP and mDendra2 emission were merged in Andor IQ2 and converted into Imaris files using a custom-made MATLAB code.

Super-Resolution 3D-SIM

Super-resolution 3D-SIM was performed as published before (Roth et al., 2015). Additional details can be found in the Supplemental Experimental Procedures.

Yeast Two-Hybrid Assay

polo, *cnb*, *plp*, and *wdr62* full-length cDNA were first cloned into pDONR221 using BP clonase. Gateway cloning technology was then used to subclone the cDNA from these entry vectors into pDEST32 (Gal4 DNA-binding domain containing destination vector) or pDEST22 (Gal4 activation domain containing destination vector) using LR Clonase (Life Technologies).

Yeast two-hybrid assays were performed using the ProQuest Two-Hybrid System (Life Technologies). pDEST32 and pDEST22 vectors containing the bait and prey cDNA, respectively, were co-transformed into the MaV203 yeast strain. The expression of the reporter genes *lacZ* and *URA3* was tested according to the manufacturer's manual.

Statistics and Sample Number

Statistical significance was calculated using the unpaired-samples Student's t test. F tests were performed first to determine the equality of variance. For each experiment, the data were collected from at least three independent brain lobes. Scored neuroblasts are shown in the figures or mentioned in the legends.

SUPPLEMENTAL INFORMATION

Supplemental Information includes Supplemental Experimental Procedures, seven figures, and seven movies and can be found with this article online at http://dx.doi.org/10.1016/j.celrep.2015.12.097.

AUTHOR CONTRIBUTIONS

A.R.N. and C.C. conceived and designed the project. A.R.N. performed the experiments with help from P.S. D.S.G. and A.R.N. generated the *wdr62*

CRISPR alleles. A.R.N., D.R.-C., and B.E. generated brain size data. A.R.N., P.S., D.R.-C., B.E., and C.C. analyzed the data. A.R.N. and C.C wrote the manuscript.

ACKNOWLEDGMENTS

We thank Tri Thanh Pham for custom-made MATLAB codes and Emmanuel Gallaud for helping with the cold assays and insightful discussions. We also thank Emmanuel Gallaud and Fiona Doetsch for critical reading of the manuscript. We are grateful to Tim Megraw, Jordan Raff, Renata Basto, Juergen Knoblich, Cayetano Gonzalez, Monica Bettencourt-Dias, Tomer Avidor-Reiss, Chris Doe, Fumio Matsuzaki, Nasser Rusan, and the Bloomington Drosophila Stock Center (NIH P40OD018537) for flies and antibodies. We thank Alexia Isabelle Loynton-Ferrand of the Imaging Core Facility (IMCF) for technical support. This work was supported by an EMBO long-term postdoctoral fellowship to P.S. (EMBO ALTF 628-2012), the Swiss National Science Foundation (SNSF; PP00P3_133658), and the Novartis Foundation for Biomedical Research. B.E. thanks Simon Sprecher for continuous support.

Received: October 15, 2015
Revised: December 10, 2015
Accepted: December 21, 2015
Published: January 21, 2016

REFERENCES

Albertson, R., and Doe, C.Q. (2003). Dlg, Scrib and Lgl regulate neuroblast cell size and mitotic spindle asymmetry. Nat. Cell Biol. *5*, 166–170.

Basto, R., Gomes, R., and Karess, R.E. (2000). Rough deal and Zw10 are required for the metaphase checkpoint in Drosophila. Nat. Cell Biol. *2*, 939–943.

Bilgüvar, K., Oztürk, A.K., Louvi, A., Kwan, K.Y., Choi, M., Tatli, B., Yalnizoğlu, D., Tüysüz, B., Cağlayan, A.O., Gökben, S., et al. (2010). Whole-exome sequencing identifies recessive WDR62 mutations in severe brain malformations. Nature *467*, 207–210.

Brand, A.H., and Livesey, F.J. (2011). Neural stem cell biology in vertebrates and invertebrates: more alike than different? Neuron *70*, 719–729.

Buszczak, M., Paterno, S., Lighthouse, D., Bachman, J., Planck, J., Owen, S., Skora, A.D., Nystul, T.G., Ohlstein, B., Allen, A., et al. (2007). The Carnegie protein trap library: a versatile tool for Drosophila developmental studies. Genetics *175*, 1505–1531.

Cabernard, C., and Doe, C.Q. (2009). Apical/basal spindle orientation is required for neuroblast homeostasis and neuronal differentiation in Drosophila. Dev. Cell *17*, 134–141.

Cabernard, C., and Doe, C.Q. (2013). Live imaging of neuroblast lineages within intact larval brains in Drosophila. Cold Spring Harb. Protoc. *2013*, 970–977.

Cai, Y., Yu, F., Lin, S., Chia, W., and Yang, X. (2003). Apical complex genes control mitotic spindle geometry and relative size of daughter cells in Drosophila neuroblast and pI asymmetric divisions. Cell *112*, 51–62.

Chen, J.-F., Zhang, Y., Wilde, J., Hansen, K.C., Lai, F., and Niswander, L. (2014). Microcephaly disease gene Wdr62 regulates mitotic progression of embryonic neural stem cells and brain size. Nat. Commun. *5*, 3885.

Cohen-Katsenelson, K., Wasserman, T., Khateb, S., Whitmarsh, A.J., and Aronheim, A. (2011). Docking interactions of the JNK scaffold protein WDR62. Biochem. J. *439*, 381–390.

Conduit, P.T., and Raff, J.W. (2010). Cnn dynamics drive centrosome size asymmetry to ensure daughter centriole retention in Drosophila neuroblasts. Curr. Biol. *20*, 2187–2192.

Conduit, P.T., Feng, Z., Richens, J.H., Baumbach, J., Wainman, A., Bakshi, S.D., Dobbelaere, J., Johnson, S., Lea, S.M., and Raff, J.W. (2014). The centrosome-specific phosphorylation of Cnn by Polo/Plk1 drives Cnn scaffold assembly and centrosome maturation. Dev. Cell *28*, 659–669.

Fu, J., and Glover, D.M. (2012). Structured illumination of the interface between centriole and peri-centriolar material. Open Biol. *2*, 120104.

Godek, K.M., Kabeche, L., and Compton, D.A. (2015). Regulation of kinetochore-microtubule attachments through homeostatic control during mitosis. Nat. Rev. Mol. Cell Biol. *16*, 57–64.

Gruber, R., Zhou, Z., Sukchev, M., Joerss, T., Frappart, P.O., and Wang, Z.Q. (2011). MCPH1 regulates the neuroprogenitor division mode by coupling the centrosomal cycle with mitotic entry through the Chk1-Cdc25 pathway. Nat. Cell Biol. *13*, 1325–1334.

Homem, C.C.F., and Knoblich, J.A. (2012). Drosophila neuroblasts: a model for stem cell biology. Development *139*, 4297–4310.

Hussain, M.S., Baig, S.M., Neumann, S., Nürnberg, G., Farooq, M., Ahmad, I., Alef, T., Hennies, H.C., Technau, M., Altmüller, J., et al. (2012). A truncating mutation of CEP135 causes primary microcephaly and disturbed centrosomal function. Am. J. Hum. Genet. *90*, 871–878.

Jakobsen, L., Vanselow, K., Skogs, M., Toyoda, Y., Lundberg, E., Poser, I., Falkenby, L.G., Bennetzen, M., Westendorf, J., Nigg, E.A., et al. (2011). Novel asymmetrically localizing components of human centrosomes identified by complementary proteomics methods. EMBO J. *30*, 1520–1535.

Januschke, J., and Gonzalez, C. (2010). The interphase microtubule aster is a determinant of asymmetric division orientation in Drosophila neuroblasts. J. Cell Biol. *188*, 693–706.

Januschke, J., Llamazares, S., Reina, J., and Gonzalez, C. (2011). Drosophila neuroblasts retain the daughter centrosome. Nat. Commun. *2*, 243.

Januschke, J., Reina, J., Llamazares, S., Bertran, T., Rossi, F., Roig, J., and Gonzalez, C. (2013). Centrobin controls mother-daughter centriole asymmetry in Drosophila neuroblasts. Nat. Cell Biol. *15*, 241–248.

Karpova, N., Bobinnec, Y., Fouix, S., Huitorel, P., and Debec, A. (2006). Jupiter, a new Drosophila protein associated with microtubules. Cell Motil. Cytoskeleton *63*, 301–312.

Lee, C.-Y., Andersen, R.O., Cabernard, C., Manning, L., Tran, K.D., Lanskey, M.J., Bashirullah, A., and Doe, C.Q. (2006). Drosophila Aurora-A kinase inhibits neuroblast self-renewal by regulating aPKC/Numb cortical polarity and spindle orientation. Genes Dev. *20*, 3464–3474.

Lerit, D.A., and Rusan, N.M. (2013). PLP inhibits the activity of interphase centrosomes to ensure their proper segregation in stem cells. J. Cell Biol. *202*, 1013–1022.

Lerit, D.A., Jordan, H.A., Poulton, J.S., Fagerstrom, C.J., Galletta, B.J., Peifer, M., and Rusan, N.M. (2015). Interphase centrosome organization by the PLP-Cnn scaffold is required for centrosome function. J. Cell Biol. *210*, 79–97.

Megraw, T.L., Sharkey, J.T., and Nowakowski, R.S. (2011). Cdk5rap2 exposes the centrosomal root of microcephaly syndromes. Trends Cell Biol. *21*, 470–480.

Morin, X., Daneman, R., Zavortink, M., and Chia, W. (2001). A protein trap strategy to detect GFP-tagged proteins expressed from their endogenous loci in Drosophila. Proc. Natl. Acad. Sci. USA *98*, 15050–15055.

Moutinho-Santos, T., Sampaio, P., Amorim, I., Costa, M., and Sunkel, C.E. (1999). In vivo localisation of the mitotic POLO kinase shows a highly dynamic association with the mitotic apparatus during early embryogenesis in Drosophila. Biol. Cell *91*, 585–596.

Nicholas, A.K., Khurshid, M., Désir, J., Carvalho, O.P., Cox, J.J., Thornton, G., Kausar, R., Ansar, M., Ahmad, W., Verloes, A., et al. (2010). WDR62 is associated with the spindle pole and is mutated in human microcephaly. Nat. Genet. *42*, 1010–1014.

Nigg, E.A., and Stearns, T. (2011). The centrosome cycle: Centriole biogenesis, duplication and inherent asymmetries. Nat. Cell Biol. *13*, 1154–1160.

Nigg, E.A., Čajánek, L., and Arquint, C. (2014). The centrosome duplication cycle in health and disease. FEBS Lett. *588*, 2366–2372.

Peel, N., Stevens, N.R., Basto, R., and Raff, J.W. (2007). Overexpressing centriole-replication proteins in vivo induces centriole overduplication and de novo formation. Curr. Biol. *17*, 834–843.

Rebollo, E., Sampaio, P., Januschke, J., Llamazares, S., Varmark, H., and González, C. (2007). Functionally unequal centrosomes drive spindle orientation in asymmetrically dividing Drosophila neural stem cells. Dev. Cell *12*, 467–474.

Roth, M., Roubinet, C., Iffländer, N., Ferrand, A., and Cabernard, C. (2015). Asymmetrically dividing Drosophila neuroblasts utilize two spatially and temporally independent cytokinesis pathways. Nat. Commun. *6*, 6551.

Roubinet, C., and Cabernard, C. (2014). Control of asymmetric cell division. Curr. Opin. Cell Biol. *31*, 84–91.

Rusan, N.M., and Peifer, M. (2007). A role for a novel centrosome cycle in asymmetric cell division. J. Cell Biol. *177*, 13–20.

Salzmann, V., Chen, C., Chiang, C.Y., Tiyaboonchai, A., Mayer, M., and Yamashita, Y.M. (2014). Centrosome-dependent asymmetric inheritance of the midbody ring in Drosophila germline stem cell division *25*, 267–275.

Singh, P., Ramdas Nair, A., and Cabernard, C. (2014). The centriolar protein Bld10/Cep135 is required to establish centrosome asymmetry in Drosophila neuroblasts. Curr. Biol. *24*, 1548–1555.

Wang, X., Tsai, J.W., Imai, J.H., Lian, W.N., Vallee, R.B., and Shi, S.H. (2009). Asymmetric centrosome inheritance maintains neural progenitors in the neocortex. Nature *461*, 947–955.

Wasserman, T. et al., 2010. A novel c-Jun N-terminal kinase (JNK)-binding protein WDR62 is recruited to stress granules and mediates a nonclassical JNK activation. 21, 117–130.

Xu, D., Zhang, F., Wang, Y., Sun, Y., and Xu, Z. (2014). Microcephaly-associated protein WDR62 regulates neurogenesis through JNK1 in the developing neocortex. Cell Rep. *6*, 104–116.

Yadlapalli, S., and Yamashita, Y.M. (2013). Chromosome-specific nonrandom sister chromatid segregation during stem-cell division. Nature *498*, 251–254.

Yamashita, Y.M., Mahowald, A.P., Perlin, J.R., and Fuller, M.T. (2007). Asymmetric inheritance of mother versus daughter centrosome in stem cell division. Science *315*, 518–521.

Yu, T.W., Mochida, G.H., Tischfield, D.J., Sgaier, S.K., Flores-Sarnat, L., Sergi, C.M., Topçu, M., McDonald, M.T., Barry, B.J., Felie, J.M., et al. (2010). Mutations in WDR62, encoding a centrosome-associated protein, cause microcephaly with simplified gyri and abnormal cortical architecture. Nat. Genet. *42*, 1015–1020.